

Road feature extraction from LANDSAT-8 operational land imager images using simplified U-Net model

Sama Lenin Kumar Reddy^{1,2}, Chandu Venkateswara Rao¹, Pullakura Rajesh Kumar²

¹Techonology and Innovation, National Remote Sensing Centre (NRSC), Indian Space Research Organization (ISRO), Hyderabad, India

²Department of Electronics and Communication Engineering, Andhra University, Vishakapatnm, India

Article Info

Article history:

Received Mar 15, 2024

Revised Sep 9, 2024

Accepted Oct 1, 2024

Keywords:

LANDSAT-8 operational land imager

Linear imaging and self-scanning sensor-4

Road feature extraction

Saturation based adaptive thresholding and morphology

Simplified U-Net

U-Net model

ABSTRACT

Automatic road feature extraction from the remote sensing (RS) imagery has a significant role in various applications such as urban planning, transportation management, and environmental monitoring. In this paper, propose a method based on the U-Net model to extract the road features from the LANDSAT-8 operational land imager (OLI) images. This method aims to extract road features in OLI images that appear as curvilinear features and roads with widths greater than 25 meters, which are mostly covered within a single pixel of the OLI resolution of multi-spectral images. The U-Net architecture is well-known for its effectiveness in image segmentation tasks. However, to optimize the complexity in the U-Net model, simplified the architecture while retaining its key components and principles. The proposed model by decreasing the convolution layers and the parameters which are involved to optimize the model called as simplified U-Net model. To train this model, the label images were generated for LANDSAT-8 OLI images, by using the saturation based adaptive thresholding and morphology (SATM) method. This reduces the efforts to draw the labels in the vector format labels and convert to raster images. The model is able to effectively generate weights, which are able to extract the road features. This model weights applied on the OLI images which covers the urban and rural areas of India, producing the satisfactory results. The experimental results with the quantitative analysis presented in the paper.

This is an open access article under the [CC BY-SA](https://creativecommons.org/licenses/by-sa/4.0/) license.



Corresponding Author:

Sama Lenin Kumar Reddy

Department of Electronics and Communication Engineering, Andhra University

Waltair Junction, Visakhapatnam, Andhra Pradesh 530003, India

Email: leninkumar438@gmail.com

1. INTRODUCTION

In recent years, remote sensing (RS) images have tremendous importance in various applications, such as disaster monitoring, town and irrigation planning, and traffic management. Specifically, roads play a crucial role in enhancing urban layout and town planning. Consequently, the automation of road feature extraction from RS images has become significantly increased worldwide [1] due to acquisition of data in the regular intervals with enough resolution of data. The main objective of this paper is to extract road features with widths greater than 25 meters. For this purpose, low-resolution (LR) operational land imager (OLI) data was selected, which includes 12 multispectral bands with a 30-meter resolution and a panchromatic band with a 15 m resolution. The swath (coverage area on the Earth) is 185 km, and the revisit period is 16 days.

The extraction of road features from RS images is a challenging task due to the complexity of spatial and spectral variations from image to image, as well as variations caused by environmental conditions. Specifically, the spatial resolution of the data is crucial for identifying feature sizes [2]. In the

images, the spectral ranges of road features change due to buildings, which have higher reflectance than the roads. If the road is located beside buildings, as in urban areas, this effect is more pronounced. Additionally, trees and their shadows also affect the spectral ranges of the roads.

Singh and Garg [3], and Herald and Roberts [4] presented analysis on the road reflectance variations, in different conditions and various ages of roads using in-situ measurements. Shahi *et al.* [5] proposed a road extraction index (REI) for WorldView-2 sensor data, based on the spectral variations in the multi-spectral bands. From these [3]–[5] the multi-spectral bands are playing an important role in the extraction of road features also. As presented in [3], [4], the presented variations of roads reflectance ranges are matches with OLI multi-spectral bands ranges, from this selected bands are short-wave infrared 1 (SWIR 1) (Band 6), near infra-red (NIR) (Band 5), and blue (Band 2) [6].

In RS images, index-based methods are popular, such as normalized difference vegetation index (NDVI) for the extraction of vegetation [7] and normalized difference water index (NDWI) [8] for the extraction of water bodies. These indices typically do not require extensive post-processing because they have significant reflectance features compared to other features. However, road features exhibit multiple variations that affect reflectance, as mentioned above. Due to this complexity, researchers have applied various methods to extract road features.

Traditional methods like edge detection, segmentation, and clustering encounter challenges in capturing diverse image features [9], machine learning techniques such as support vector machines (SVM) [10] and Markov random fields (MRF) [6] have shown notable performance. Current road detection methods often rely on pixel-level segmentation or classification. For instance, Song and Civco [10] proposed a two-phase model involving SVM for initial pixel classification and a segmentation algorithm to refine road pixels and generate the road regions.

Das *et al.* [11] presented analysis on various methodologies for road feature extraction as well analyzed on the multi-spectral satellite images, utilizing distinct spectral contrast and locally linear trajectory features. Trained probabilistic SVM on urban or suburban samples, coupled with dominant singular measure for trajectory detection and an optimization framework to achieve the accuracy. Zhang and Couloigner [12] proposed a two-step method involving initial image segmentation into clusters, followed by a fuzzy logic classifier using angular texture signature features to identify road clusters. Similarly, Wegner *et al.* [13] introduced a road detection approach based on a higher-order conditional random field (CRF) model. This model represents road prior using higher-order cliques, connected sets of super-pixels along straight line segments, seamlessly integrated into the CRF classifier for effective road detection. The methodologies employ a multi-stage process for extracting road features, complemented by post-processing for enhanced accuracy.

Artificial intelligence (AI), particularly through deep learning and convolution neural networks (CNN), has gained significance in road detection from satellite images. CNN, with its robust capabilities in pixel classification and object detection [14], has demonstrated with high accuracy in various fields, including RS images [15]. Recently, CNN has been effectively applied in the automatic control and classification of medical images, utilizing network architecture U-Net [16]. Ronneberger *et al.* introduced the U-Net model [16], which has since become a popular choice for various image segmentation tasks, specifically focus on road extraction from RS imagery [17]–[20] of high resolution images which have the more pixels for road features. SegNet [21] model presented for the automatic road feature extraction, utilizes prior probability for pixel classification. The encoder employs convolution-pooling for down-sampling, and the decoder uses deconvolution and up-sampling based on the transmission index obtained from the encoder. Li *et al.* [22] introduced DeepUNet, an extension of the original U-Net model, emphasizing the significance of precise road segmentation. DeepUNet, a deep fully convolutional network, combines U-Net and deep convolutional network strengths for pixel-level road extraction. Evaluated on road extraction datasets and compared with state-of-the-art methods, DeepUNet demonstrates superior performance in accurately segmenting road features at the pixel level, surpassing others in accuracy and robustness. These methods also highlight the challenges associated with road detection, such as varying road widths, complex road structures, and diverse road appearances. The U-Net architecture is presented as a solution to address these challenges. The literature demonstrates the extraction of road features from high-resolution (HR) images, whereas this paper presents findings based on LR RS images.

The U-Net architecture has positioned itself as one of the best methods for extracting road features from RS imagery. Its effectiveness in this domain provides a robust foundation for ongoing research and diverse applications in the field. The increasing interest in employing deep neural network-based approaches for road feature extraction is evident, with various architectures and methodologies being explored to enhance accuracy and efficiency. In the existing literature, most researchers have concentrated on road feature extraction from aerial, very high-resolution (VHR), and HR images. This study, however, aims to explore the potential of extracting road features from OLI images.

2. PROPOSED METHOD

The paper introduces a simplified U-Net model designed for extracting road features from OLI images, following the U-Net architecture [16]. It is crucial to emphasize that effective training of supervised deep learning (DL) models requires a comprehensive training dataset to ensure accurate feature extraction. As aforementioned in section 1 the OLI sensor includes 9 optical bands and 2 thermal bands. The road feature extraction model focuses on three specific bands for input: blue, NIR, and SWIR 1. These bands are chosen due to their high reflectance characteristics for asphalt in the NIR and SWIR spectral ranges [3], [4]. By utilizing these selected bands, the model effectively captures and analyses pertinent information for road feature extraction.

In the training set, both the original images and the corresponding label images are included. The label image were generated by the saturation based thresholding and morphology (SATM) method [6] from the OLI RS image. In label or train image, road pixels are assigned as a value of ‘1’, while non-road pixels are assigned as a value of ‘0’. This labelling process allows the model to learn and differentiate between road and non-road regions during training.

Data augmentation is a randomized method used to select augmented data for the model. This involves applying diverse transformations, such as rotating input images at angles ranging from 15° to 90° with 15° intervals, and generating mirror images by horizontal flipping [23]. These augmentations enhance the diversity of training samples, thereby improving the model’s generalization and performance. The approach allows the model to learn from a broader and more varied set of training samples, which is particularly advantageous in scenarios with limited labelled data. The rotation and mirroring transformations enable the model to better recognize objects from different viewpoints and orientations, enhancing its ability to accurately generalize and classify unseen images.

2.1. Model architecture

The model presented in these papers adopts a U-Net architecture, featuring contracting (down-block) and expanding (up-block) layers. The input image size is 640×640×3, where 640×640 represents the image dimensions, and 3 denotes the number of bands. Referred to as the simplified U-Net, its architecture is illustrated in Figure 1.

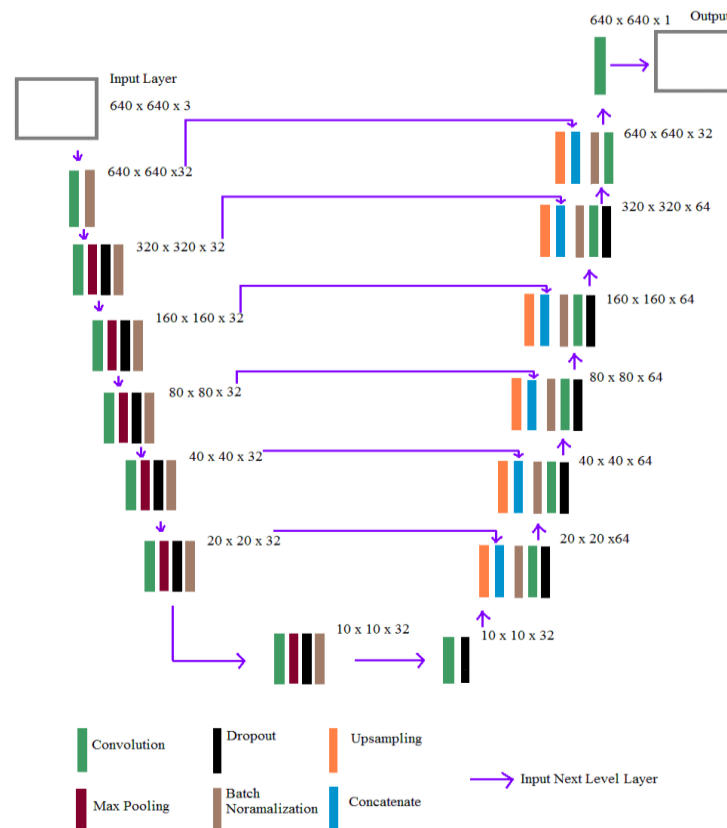


Figure 1. Simplified U-Net model architecture view

In the down-block, each level incorporates a single convolution layer with a filter size of 32. These 3×3 kernel size convolution layers capture correlations among neighboring pixels, enabling the model to identify sharp edges and accurately predict features. The rectified linear unit (ReLU) activation function is applied after each convolution layer to rectify values below 0 and pass the remaining weights to the next layer. Batch normalization layers at each level normalize the detected feature values from the convolution layer. Additionally, max-pooling layers of a size of 2 are included at each level to reduce the image size. Dropout layers with a rate of 0.25 are employed at each level to address over-fitting concerns during prediction. The down-block consists of a total of 6 levels, with the output image size decreasing by a factor of 2 at each level. For instance, at level 6, the image size becomes 10×10.

In the up-block, the goal is to restore the original image size through up-sampling, enhancing the resolution of feature maps. Each level involves concatenating the output from the previous layer with a layer of similar size. Like the down-block, the up-block has 6 levels to restore the original image size, with each level containing a single convolution layer featuring 64 filters, followed by batch normalization to normalize feature values.

The output of the convolution layer in the Up-block undergoes a sigmoid activation function to obtain probabilities (weights) for all possible classes. The model is optimized using the Adam optimizer [24] with a binary cross-entropy loss function, with batch size 2 and 10,000 epochs and the learning rate is automatically adjusted based on the weights. Training utilizes images with extracted roads from [5], resulting in a training accuracy of 98.52%.

The proposed simplified U-Net model, featuring an encoder-decoder network with skip connections, is designed to capture both global and local contextual information. Utilizing convolutional and pooling layers, the encoder extracts hierarchical features from the input OLI images. The decoder then reconstructs road feature maps at different scales, preserving spatial details and accurately delineating road boundaries.

3. RESULTS AND DISCUSSION

3.1. Datasets

The experiments were carried out on the OLI images covering the areas of Hyderabad in Figures 2(a) to 2(f), Chennai in Figures 3(a) and 3(b), and Bangalore in Figures 4(a) and 4(b), India using the proposed model. The label or training samples were extracted by the SATM method [6] from Figure 2(a). The size of the images is 3145×3045×3, which reduces the manual effort required to draw the labels in vector format and convert them to raster format. These images (original and label) were cropped (3/4 of the original image) into multiple blocks (300 labels) with a size of 640×640×3. A random augmentation technique, as mentioned in the section proposed, was used to generate 300 samples. The model was trained with the image in Figure 2(a) only, while Figures 3(a) and 4(a) were utilized as test case images.

Despite variations in datasets stemming from different acquisition dates and atmospheric conditions, the model excels in accurately inferring road features. The extracted road features undergo a meticulous comparison with manually digitized road features [11], and the corresponding accuracy metrics, including precision, recall, and F1-score [25], are presented in Tables 1 and 2. Specifically, Table 1 showcases the accuracy of the proposed model on the OLI images covering the aforementioned areas. The performance evaluation for one of the areas, specifically the Hyderabad OLI image, was utilized for detailed performance analysis. The results are systematically tabulated in Table 2.

The extracted road features by the proposed model from Figure 2(a) are shown in Figure 2(b). It was observed that a greater number of road features were extracted compared to manually drawn roads, as well as the SATM method and U-Net [16], [22]. Gaps were identified between the road features due to roads being covered by trees, multi-story buildings, and their shadows, which affect road reflectance values. Additionally, the width of the roads was greater than 25 meters. Unconnected road features with fewer pixels (<500 pixels) were eliminated using connected component analysis. For gaps between road features <50 pixels, the circle window method with a radius of 50 pixels was employed to fill the gaps, resulting in the image shown in Figure 2(c).

The road features were manually drawn using QGIS at a 1:50,000 scale, and road vector layers were overlaid on the predicted road features by the proposed model, as shown in Figure 2(d). It was observed that minor roads less than 25 meters were able to be extracted when they were free from occlusions. To compare the predicted roads, the DeepUNet model [22] was employed to predict the road features, and the same method was used to eliminate unwanted pixels, as shown in Figure 2(e). Using the QGIS tool, an overlay of road features predicted by the proposed model and the DeepUNet model for visual comparison is shown in Figure 2(f). It was observed that the proposed model predicted more road features, highlighted in the image with ellipses, although a few road pixels predicted by DeepUNet were missing.

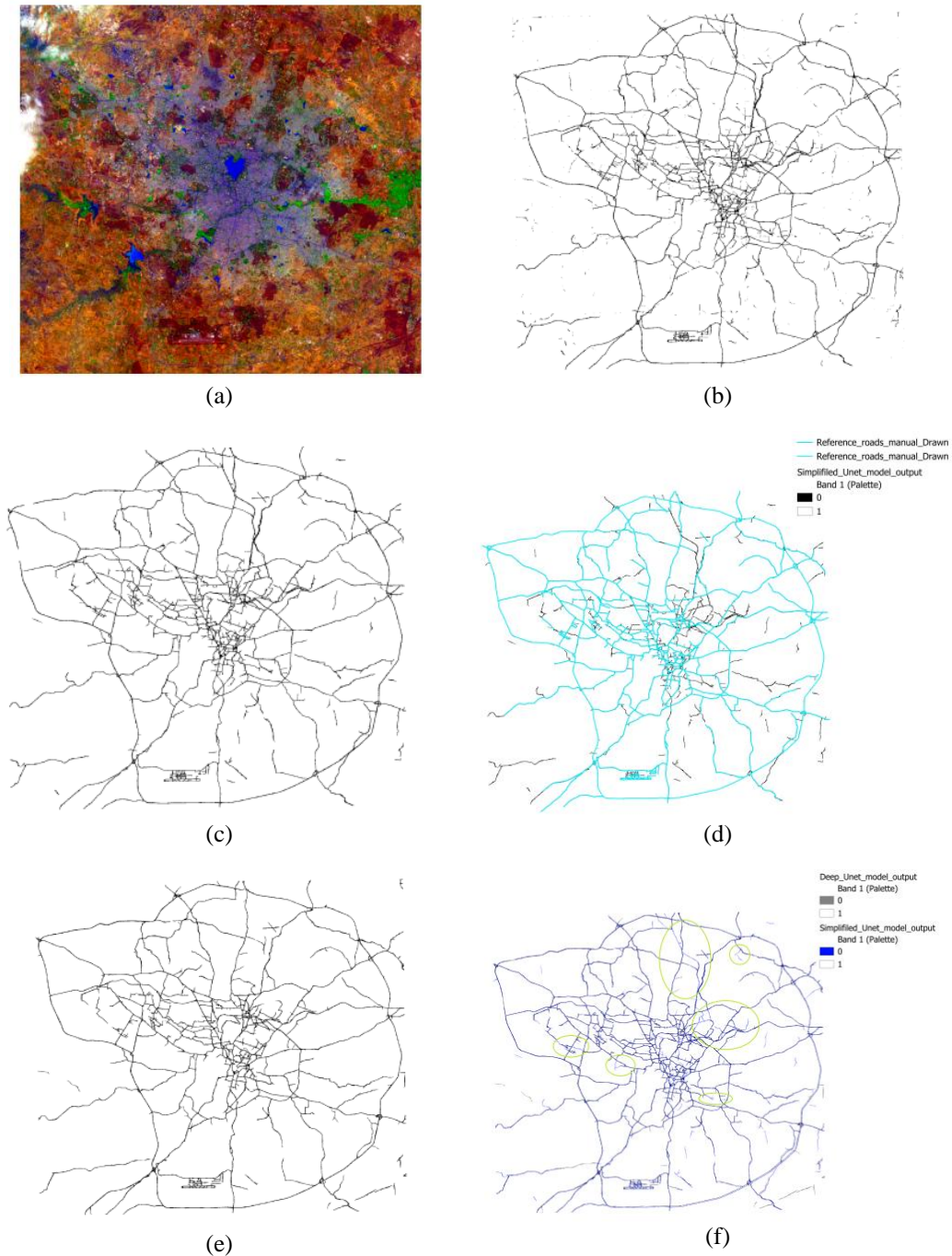


Figure 2. Road features extracted by simplified U-Net from OLI Image which covers Hyderabad area is (a) OLI image (B6-SWIR-1, B5-NIR, B2-Blue) (Hyderabad), (b) roads predicted by the proposed model, (c) road features smoothed by morphological operators, (d) reference vector layer (manual drawn) overlay on the proposed model output, (e) road features extraction using Deep U-Net [22], smoothed by morphological operators, and (f) overlay of extracted road features by Deep U-Net and simplified U-Net model

In a similar vein, the model was employed to extract road features from the test case images presented in Figure 3(a) and Figure 4(a), which are not part of the training or validation datasets. The resulting road features are vividly illustrated in the corresponding images of Figure 3(b) and Figure 4(b). From these results, it was observed that the model was able to predict a good amount of road pixels, but there were more gaps between the road pixels. This could be mitigated by training the model with a diverse set of road pixel labels, including various types of road pixels and time series data, which may improve accuracy in test cases.

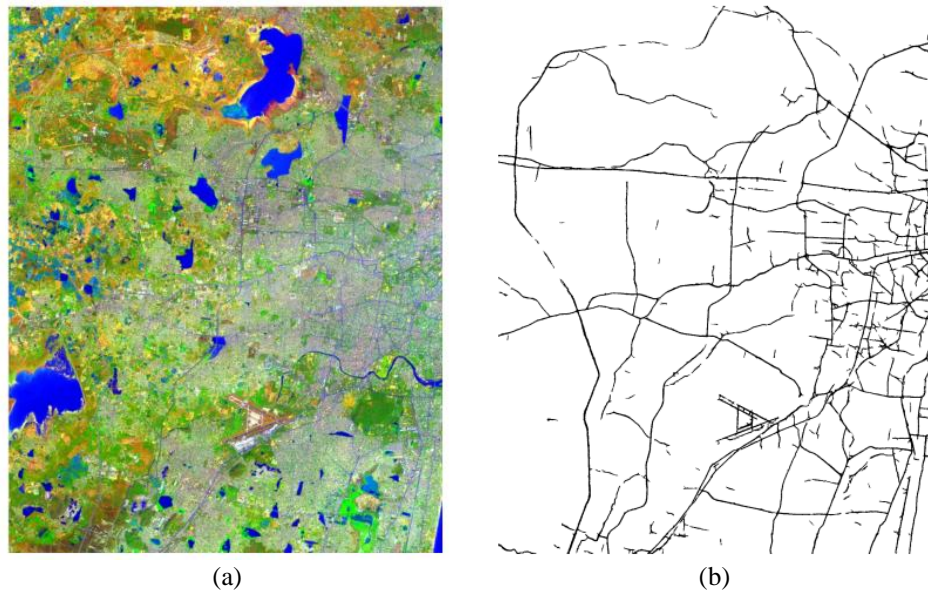


Figure 3. Road features extracted by simplified U-Net from OLI image which covers Chennai area is (a) OLI Image (B6-SWIR-1, B5-NIR, B2-Blue) (Chennai) and (b) road features predicted by the proposed model

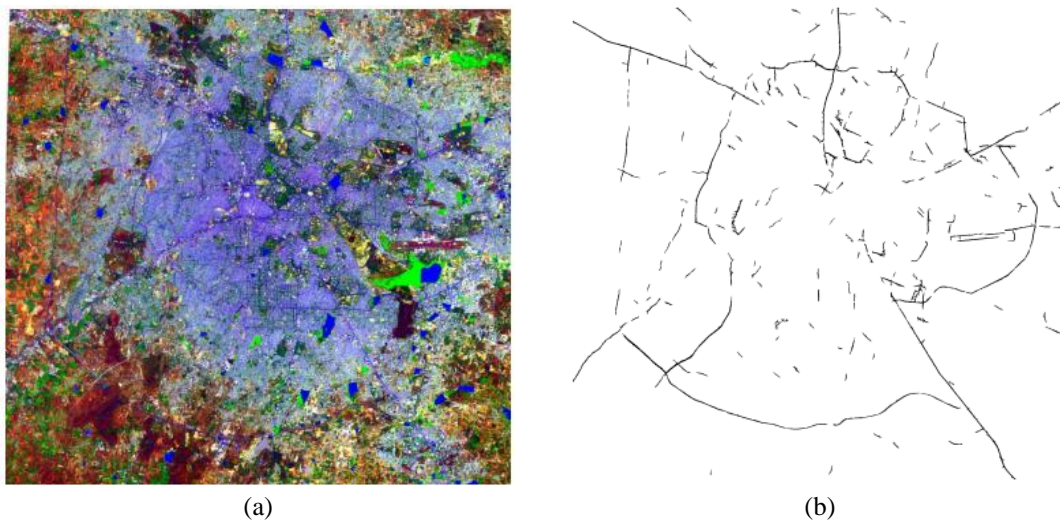


Figure 4. Road features extracted by simplified U-Net from OLI image which covers Bangalore area is (a) OLI image (B6-SWIR-1, B5-NIR, B2-Blue) (Bangalore) and (b) road features extracted by simplified U-Net from OLI image which covers Bangalore area

Table 1. Accuracy of proposed model

Datset	Precision	Recall	F1-Score
Hyderabad	90.28	99.38	94.16
Chennai	92.16	99.41	95.65
Bangalore	89.97	83.56	86.64

Table 2. Performance evaluation of models on Figure 2(a) (Hyderabad)

Datset	Precision	Recall	F1-Score
SATM [6]	75.27	98.38	85.29
U-Net [16]	87.37	99.16	92.35
DeepUNet [22]	88.53	98.86	93.41
Proposed model	90.28	99.38	94.16

The methodology was applied to the linear imaging and self-scanning sensor-4 (LISS-4) data obtained from ResourceSat-2, provided by NRSC/ISRO, and downloaded through ‘BhooNidhi’ [26]. The LISS-4 sensor comprises three bands (near-infrared, red, and green) with a spatial resolution of 5.8 meters [27] and a coverage swath of 70 kilometers. LISS-4 provides high-resolution imagery, covering a portion of Hyderabad as shown in Figure 5(a). Benefiting from this high resolution, the proposed model is able to extract road features with widths less than 5 meters, as depicted in Figure 5(b).

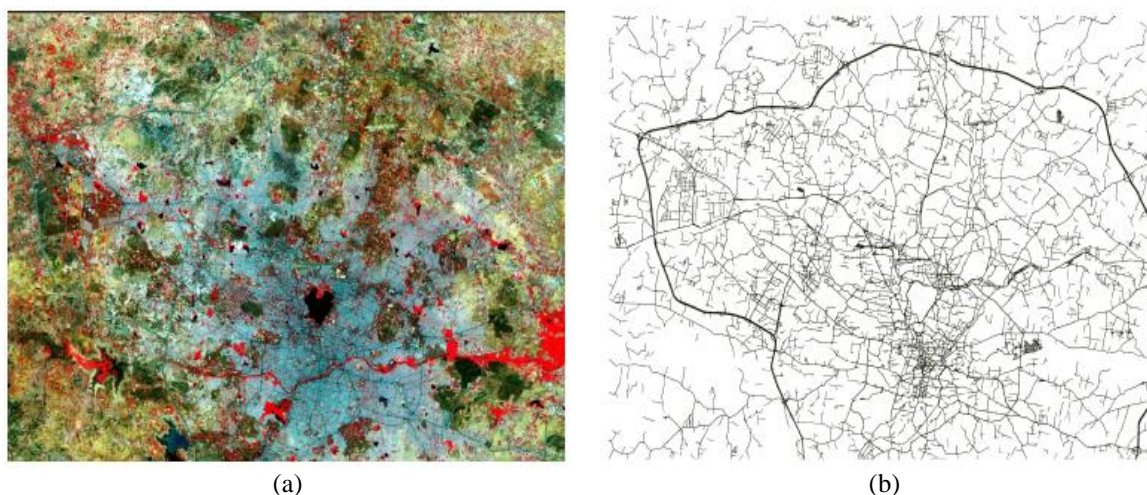


Figure 5. Road features extraction from ResourceSat-2 LISS-4 sensor which covers Hyderabad area is (a) ResourceSat-2 LISS-4 Image (B4-NIR, B3-Red, B2-Green) (Hyderabad) and (b) road features extracted by simplified U-Net from OLI image

4. CONCLUSION

This paper presents automatic road feature extraction from OLI images using the proposed model, the simplified U-Net. The model utilizes labeled data obtained by the SATM method, reducing the manual effort required to create label images. It achieved improved accuracy for datasets covering the areas of Hyderabad (94.16%), Chennai (95.65%), and Bangalore (86.64%), with an average accuracy of 92.15%. In the results, gaps between road pixels were observed due to occlusions by trees and multi-story buildings adjacent to the roads, as well as road widths less than 25 meters. As future work to further improve accuracy, the model could benefit from training with a greater variety and number of road labels, including manually drawn features. Experimentation with LISS-4 imagery demonstrates the model’s proficiency in extracting road features, suggesting further exploration as a prospective avenue for future work. Moreover, there is potential to extend this research by incorporating Sentinel-2 and other various sensor data sources.

ACKNOWLEDGEMENTS

We wish to express our sincere gratitude to National Remote Sensing Centre and Bhoonidhi for data and their encouragement and guidance in bringing out this publication.




REFERENCES

- [1] J. Wang and Q. Zhang, “Applicability of a gradient profile algorithm for road network extraction - Sensor, resolution and background considerations,” *Canadian Journal of Remote Sensing*, vol. 26, no. 5, pp. 428–439, 2000, doi: 10.1080/07038992.2000.10855274.
- [2] S. Benjamin and L. Gaydos, “Spatial resolution requirements for automated cartographic road extraction,” *Photogrammetric Engineering & Remote Sensing*, vol. 56, no. 1, pp. 93–100, 1990.
- [3] P. P. Singh and R. D. Garg, “Study of spectral reflectance characteristics of asphalt road surface using geomatics techniques,” in *Proceedings of the 2013 International Conference on Advances in Computing, Communications and Informatics, ICACCI 2013*, 2013, pp. 516–520, doi: 10.1109/ICACCI.2013.6637225.
- [4] M. Herold and D. Roberts, “Spectral characteristics of asphalt road aging and deterioration: Implications for remote-sensing applications,” *Applied Optics*, vol. 44, no. 20, pp. 4327–4334, 2005, doi: 10.1364/AO.44.004327.
- [5] K. Shahi, H. Z. M. Shafri, E. Taherzadeh, S. Mansor, and R. Muniandy, “A novel spectral index to automatically extract road networks from WorldView-2 satellite imagery,” *Egyptian Journal of Remote Sensing and Space Science*, vol. 18, no. 1,




- pp. 27–33, 2015, doi: 10.1016/j.ejrs.2014.12.003.
- [6] S. L. K. Reddy, C. V. Rao, P. Rajesh Kumar, R. V. G. Anjaneyulu, and B. Gopala Krishna, “An index based road feature extraction from LANDSAT-8 OLI images,” *International Journal of Electrical and Computer Engineering*, vol. 11, no. 2, pp. 1319–1336, 2021, doi: 10.11591/ijece.v11i2.pp1319-1336.
- [7] M. S.K., “The use of the normalized difference water index (NDWI) in the delineation of open water features,” *International Journal of Remote Sensing*, vol. 17, no. 7, pp. 1425–1432, 1996.
- [8] G. M. Gandhi, S. Parthiban, N. Thummalu, and A. Christy, “Ndvi: vegetation change detection using remote sensing and GIS - a case study of vellore district,” *Procedia Computer Science*, vol. 57, pp. 1199–1210, 2015, doi: 10.1016/j.procs.2015.07.415.
- [9] R. V. K. Reddy, K. P. Raju, M. J. Kumar, L. R. Kumar, P. R. Prakash, and S. S. Kumar, “Comparative analysis of common edge detection algorithms using pre-processing technique,” *International Journal of Electrical and Computer Engineering*, vol. 7, no. 5, pp. 2574–2580, 2017, doi: 10.11591/ijece.v7i1.pp2574-2580.
- [10] M. Song and D. Civco, “Road extraction using SVM and image segmentation,” *Photogrammetric Engineering and Remote Sensing*, vol. 70, no. 12, pp. 1365–1371, 2004, doi: 10.14358/PERS.70.12.1365.
- [11] S. Das, T. T. Mirmalinee, and K. Varghese, “Use of salient features for the design of a multistage framework to extract roads from high-resolution multispectral satellite images,” *IEEE Transactions on Geoscience and Remote Sensing*, vol. 49, no. 10 PART 2, pp. 3906–3931, 2011, doi: 10.1109/TGRS.2011.2136381.
- [12] Q. Zhang and I. Couloigner, “Benefit of the angular texture signature for the separation of parking lots and roads on high resolution multi-spectral imagery,” *Pattern Recognition Letters*, vol. 27, no. 9, pp. 937–946, 2006, doi: 10.1016/j.patrec.2005.12.003.
- [13] J. D. Wegner, J. A. Montoya-Zegarra, and K. Schindler, “A higher-order CRF model for road network extraction,” in *Proceedings of the IEEE Computer Society Conference on Computer Vision and Pattern Recognition*, 2013, pp. 1698–1705, doi: 10.1109/CVPR.2013.222.
- [14] I. Sevo and A. Avramovic, “Convolutional neural network based automatic object detection on aerial images,” *IEEE Geoscience and Remote Sensing Letters*, vol. 13, no. 5, pp. 740–744, 2016, doi: 10.1109/LGRS.2016.2542358.
- [15] E. Maggiori, Y. Tarabalka, G. Charpiat, and P. Alliez, “Convolutional neural networks for large-scale remote-sensing image classification,” *IEEE Transactions on Geoscience and Remote Sensing*, vol. 55, no. 2, pp. 645–657, 2017, doi: 10.1109/TGRS.2016.2612821.
- [16] O. Ronneberger, P. Fischer, and T. Brox, “U-net: convolutional networks for biomedical image segmentation,” *Lecture Notes in Computer Science (including subseries Lecture Notes in Artificial Intelligence and Lecture Notes in Bioinformatics)*, vol. 9351, pp. 234–241, 2015, doi: 10.1007/978-3-319-24574-4_28.
- [17] N. Y. Q. Abderrahim, S. Abderrahim, and A. Rida, “Road segmentation using u-net architecture,” in *Proceedings - 2020 IEEE International Conference of Moroccan Geomatics, MORGEO 2020*, 2020, pp. 1–4, doi: 10.1109/Morgeo49228.2020.9121887.
- [18] M. J. Khan and P. P. Singh, “Advanced road extraction using CNN-based U-net model and satellite imagery,” *e-Prime - Advances in Electrical Engineering, Electronics and Energy*, vol. 5, p. 100244, Sep. 2023, doi: 10.1016/j.prime.2023.100244.
- [19] X. Yang, X. Li, Y. Ye, R. Y. K. Lau, X. Zhang, and X. Huang, “Road detection and centerline extraction via deep recurrent convolutional neural network U-net,” *IEEE Transactions on Geoscience and Remote Sensing*, vol. 57, no. 9, pp. 7209–7220, Sep. 2019, doi: 10.1109/TGRS.2019.2912301.
- [20] V. Chaudhary, P. K. Buttar, and M. K. Sachan, “Satellite imagery analysis for road segmentation using U-net architecture,” *The Journal of Supercomputing*, vol. 78, no. 10, pp. 12710–12725, Jul. 2022, doi: 10.1007/s11227-022-04379-6.
- [21] V. Badrinarayanan, A. Kendall, and R. Cipolla, “Segnet: a deep convolutional encoder-decoder architecture for image segmentation,” *IEEE Transactions on Pattern Analysis and Machine Intelligence*, vol. 39, no. 12, pp. 2481–2495, Dec. 2017, doi: 10.1109/TPAMI.2016.2644615.
- [22] R. Li *et al.*, “DeepUNet: a deep fully convolutional network for pixel-level sea-land segmentation,” *IEEE Journal of Selected Topics in Applied Earth Observations and Remote Sensing*, vol. 11, no. 11, pp. 3954–3962, Nov. 2018, doi: 10.1109/JSTARS.2018.2833382.
- [23] C. Shorten and T. M. Khoshgoftaar, “A survey on image data augmentation for deep learning,” *Journal of Big Data*, vol. 6, no. 1, 2019, doi: 10.1186/s40537-019-0197-0.
- [24] D. P. Kingma and J. Ba, “Adam: A Method for Stochastic Optimization,” *arXiv:1412.6980*, Dec. 2014.
- [25] C. Heipke, H. Mayer, C. Wiedemann, and O. Jamet, “Evaluation of automatic road extraction,” *International Archives of Photogrammetry and Remote Sensing*, vol. 32, pp. 47–56, 1997.
- [26] NRSC/ISRO, “LISS-IV data – ResourceSat-2,” *bhoonidhi.nrsc.gov.in*, <https://bhoonidhi.nrsc.gov.in/bhoonidhi/index.html> (accessed Mar 5, 2024).
- [27] S. Rajesh, S. Arivazhagan, K. P. Moses, and R. Abisekaraj, “Land cover/land use mapping using different wavelet packet transforms for LISS iv madurai imagery,” *Journal of the Indian Society of Remote Sensing*, vol. 40, no. 2, pp. 313–324, Jun. 2012, doi: 10.1007/s12524-011-0154-7.

BIOGRAPHIES OF AUTHORS






Sama Lenin Kumar Reddy    M.Tech. degree in digital communications from Kakatiya University (KU), India, in 2013, and working towards Ph.D. in Andhra University, Visakhapatnam, India. He was former Senior Research Fellow (SRF) at National Remote Sensing Centre (NRSC), Indian Space Research Organization (ISRO), Hyderabad, India. His current areas of research interest are image processing, pattern recognition, visual perception and computational intelligence. He can be contacted at email: leninkumar438@gmail.com.



Chandu Venkateswara Rao    former scientist, NRSC, ISRO, Hyderabad, India. He received Ph.D. in image processing from JNTU Hyderabad in 2010 and also completed Three Ph.D. thesis under his guidance (currently guiding Two students) and several M.Tech. students. He has published about 100 papers in international and national journals including conferences. His current areas of research interest are digital image processing, visual perception, computational intelligence and pattern recognition. He can contacted at email: cvrao2018@gmail.com.



Pullakura Rajesh Kumar    received PhD from Andhra University, Visakhapatnam, 2006. Currently, working as a professor at Andhra University in the Department of Electronics and Communication Engineering. He has more than 25 years of teaching and 10 years of research experience. His current areas of research interest are image processing, signal processing and antenna theory. He can contacted at email: rajeshauce@gmail.com.